BMC Medical Genomics

RESEARCH

Open Access

Molecular mechanisms underlying the co-pathogenesis of abdominal aortic aneurysm and rheumatoid arthritis: evidence based on bioinformatics analysis and clinical data

Youfu Wang[1,2], Ling Zhang[1], Wenhong Jiang[1], Quanxing Kuang[1] and Xiao Qin[1*]

Abstract

Background The incidence of abdominal aortic aneurysm (AAA) has been reported to be associated with rheumatoid arthritis (RA). This research aimed to analyze the co-pathogenesis of AAA and RA through bioinformatics and clinical data.

Methods Microarray and single-cell RNA sequencing (scRNA-seq) datasets for AAA and RA were obtained from the Gene Expression Omnibus (GEO). Differentially expressed genes (DEGs) were identified using R software (v4.2.2), followed by enrichment analyses. Hub genes were identified via the STRING database and Cytoscape software (v3.10.1). An immune cell infiltration analysis was conducted to identify key immune cell types associated with AAA and RA. Hub genes and key immune cell types were further validated using scRNA-seq datasets. NetworkAnalyst and the Drug Signature Database (DSigDB) were employed to explore the associations of hub genes with related diseases, miRNAs, transcription factors (TFs), drugs, and drug targets. Additionally, peripheral blood samples from 629 clinical patients were collected to validate the results of the immune cell infiltration analysis.

Results The AAA and RA dataset revealed 61 common DEGs, including 20 upregulated and 41 downregulated genes. Three hub genes were screened from the common DEGs, and ITK was validated as hub gene in both AAA and RA datasets. Immune infiltration analysis revealed significant upregulation of monocytes in both AAA and RA, positively correlated with ITK expression. This was validated by scRNA-seq datasets confirming elevated ITK levels in monocytes. A total of eighteen related diseases, ten target miRNAs, eight TFs, and the top ten drugs and drug targets associated with ITK were identified. Analysis of clinical data revealed that monocyte levels were significantly elevated in patients with AAA and RA.

Conclusions Our study suggests that ITK may serve as a potential biomarker involved in the co-pathogenesis of AAA and RA. Moreover, monocytes appear to play an important role in this process. The regulatory network constructed for ITK may offer preliminary insights for future research.

*Correspondence:
Xiao Qin
dr_qinxiao@hotmail.com

Full list of author information is available at the end of the article

© The Author(s) 2025. **Open Access** This article is licensed under a Creative Commons Attribution-NonCommercial-NoDerivatives 4.0 International License, which permits any non-commercial use, sharing, distribution and reproduction in any medium or format, as long as you give appropriate credit to the original author(s) and the source, provide a link to the Creative Commons licence, and indicate if you modified the licensed material. You do not have permission under this licence to share adapted material derived from this article or parts of it. The images or other third party material in this article are included in the article's Creative Commons licence, unless indicated otherwise in a credit line to the material. If material is not included in the article's Creative Commons licence and your intended use is not permitted by statutory regulation or exceeds the permitted use, you will need to obtain permission directly from the copyright holder. To view a copy of this licence, visit http://creativecommons.org/licenses/by-nc-nd/4.0/.

Keywords Abdominal aortic aneurysm, Rheumatoid arthritis, Co-pathogenesis, Bioinformatics, Immune cell infiltration analysis

Introduction

Abdominal aortic aneurysm (AAA) is a dilated arterial disease caused by decreased elasticity and abnormal dilatation of the abdominal aortic wall, and the main risk factors for AAA include male sex, smoking, old age, hypertension, and hypercholesterolemia [1]. The prevalence of AAA has increased progressively in the last two decades with the aging of the population, with an overall change from 1.3% to 8.9%, and the mortality rate due to ruptured AAA ranges between 65% and 85% [2]. Current research suggests that the pathogenesis of AAA is associated with inflammation, immune cell infiltration, cytokine activation, and tissue plasminogen activator [3, 4].

Rheumatoid arthritis (RA) is an inflammatory disease of the joints caused by dysfunction of the immune system that potentially leads to cardiovascular diseases and lung tissue damage [5]. The global incidence of this disease ranges from 0.5% to 1% [5]. The pathogenesis of RA is complex and is currently speculated to be associated with immune regulatory factors, autoantibodies, and immune cell infiltration, including rheumatoid factor, human leukocyte antigen, and anti-citrullinated protein antibody [6]. In the blood of RA patients, antibodies can form immune complexes within the joint cavity, which can activate immune cells through different pathways, prompting increased secretion of chemokines and cytokines, causing an enhanced immune response, and ultimately leading to the destruction of the joint cavity [7, 8].

Vascular involvement has been recognized as a major contributor to increased mortality in RA patients, accounting for nearly 40% of deaths [9]. Studies have shown that the incidence of AAA in RA patients is significantly higher than in the general population, which may be related to elevated pro-inflammatory cytokines and increased oxidative stress leading to endothelial cell injury [10, 11]. Moreover, existing research suggests that RA and AAA may share certain pathogenic mechanisms [12]. However, systematic investigations into the shared genes and immune cells underlying their comorbidity remain scarce, and the mechanisms of pathogenesis are still unclear.

In this context, we downloaded RA and AAA transcriptomic datasets as well as single-cell RNA-seq (scRNA-seq) data from the GEO database and employed bioinformatics approaches to identify hub genes and relevant immune cell populations involved in the co-pathogenesis of AAA and RA. We further screened for miRNAs and transcription factors (TFs) associated with these hub genes and related diseases, while also exploring potential therapeutic drugs and targets. The flowchart of the research is shown in Fig. 1.

Methods

GEO data acquisition

Six microarray datasets and three scRNA-seq datasets human gene datasets were obtained from the Gene Expression Omnibus database (GEO, http://www.ncbi.nlm.nih.gov/geo). All datasets were derived from human tissue samples. The microarray datasets included three AAA datasets (GSE47472, GSE57691, and GSE232911) and three RA datasets (GSE97779, GSE1919, and GSE55457). The GSE47472 and GSE97779 datasets were used as test datasets for analyzing the differentially expressed genes (DEGs), while the GSE57691, GSE232911, GSE1919, and GSE55457 datasets were used as validation datasets for the verification of the analysis results. The scRNA-seq datasets included one AAA dataset (GSE166676) and two RA datasets (GSE200815 and GSE246416). The two RA scRNA-seq datasets, both based on the same sequencing platform (GPL24676), were merged for subsequent analysis.

Preprocessing and analysis of scRNA-Seq data

We used the Read10X function to import the raw data and performed scRNA-seq data analysis on AAA and RA patients, as well as healthy controls, using the Seurat package (v5.0). During quality control, cells with more than 10% mitochondrial gene content were excluded. The data were then normalized using the NormalizeData function. Using the FindVariableFeatures function, the top 2,000 highly variable genes were identified in each sample for downstream analysis. Principal component analysis was performed using the RunPCA function, and the top 50 principal components were used to construct a shared nearest neighbor graph. Cell clustering was carried out using the FindNeighbors and FindClusters functions. Cell type annotation was performed using the SingleR R package (V2.2.0) based on known marker genes, and dimensionality reduction and visualization were conducted using the RunUMAP function. To explore the expression distribution of key genes across different cell types, we examined the expression levels of candidate hub genes across the identified clusters. Violin plots were generated using the VlnPlot function to visualize their distribution across immune cell types. Additionally, DEGs in cell populations with high ITK expression were subjected to enrichment analyses using the clusterProfiler R package (V4.0.5). The main enrichment results were visualized using bar plots and bubble plots.

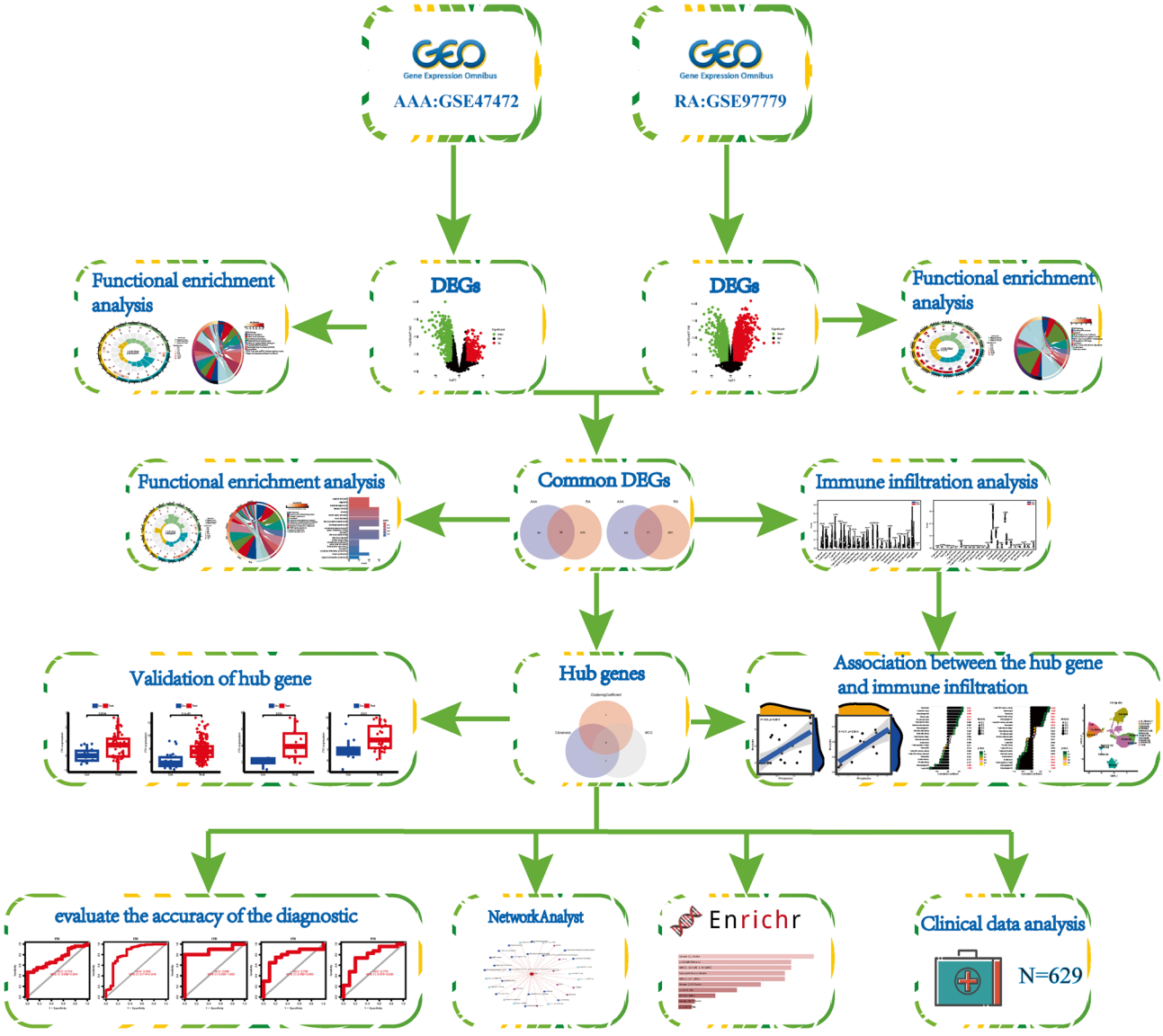


Fig. 1 The flowchart of the study procedure

Clinical data acquisition

This study was approved by the Ethics Committee of the First Affiliated Hospital and the Fourth Affiliated Hospital of Guangxi Medical University. A total of 625 participants were enrolled from these two hospitals between December 2021 and December 2023, including 216 patients with AAA, 200 patients with RA, and 213 healthy individuals. The inclusion criteria for AAA patients were: (1) age over 18 years; (2) a maximum abdominal aortic diameter greater than 5 cm confirmed by computed tomography. Patients with infectious AAA or pseudoaneurysm were excluded. The inclusion criteria for RA patients were: (1) age over 18 years; (2) fulfillment of the 2010 diagnostic criteria established by the American College of Rheumatology or the European League Against Rheumatism, with exclusion of individuals with other autoimmune or infectious diseases. Healthy controls were recruited from individuals undergoing routine outpatient physical examinations. Peripheral venous blood (5–10 mL) was collected from all participants using ethylenediaminetetraacetic acid anticoagulant tubes under sterile conditions and processed within 2 h of collection. Whole blood samples were analyzed using an automated hematology analyzer.

Identification of DEGs

All the datasets were first normalized using the normalizeBetweenArrays function from the limma package (v3.52) in R software (v4.2.2), and DEGs were then screened from the AAA dataset GSE47472 and the RA dataset GSE97779 using the same R package [13]. The common DEGs between AAA and RA patients were

subsequently identified via the Venn R package (v1.12) [14]. DEGs were screened with |logFC| >0.585 (at least 1.5-fold change in gene expression) and an adjusted p-value < 0.05 [15].

Functional enrichment analysis of DEGs

The DEGs identified from the AAA and RA datasets were subjected to Gene Ontology (GO) and Kyoto Encyclopedia of Genes and Genomes (KEGG) enrichment analysis using the clusterProfiler package (v4.6.2), implemented in R software (v4.2.2) [16, 17]. Gene annotation and identifier conversion were performed using the org.Hs.eg.db package (v3.16.0). Visualization of enrichment results was performed using the enrichplot (v1.18.4) and ggplot2 (v3.4.2) packages. In addition, the common DEGs identified in both AAA and RA datasets were subjected to GO, KEGG, and Disease Ontology (DO) enrichment analyses using the clusterProfiler (v4.6.2) and DOSE (v3.26.1) packages [18]. A p-value of < 0.05 was defined as the threshold of significance.

Identification of hub genes

The common DEGs from the AAA and RA datasets were imported into the STRING database (https://cn.string-db.org). Protein–protein interaction networks were constructed for common DEGs by defining the minimum interaction score as 0.400, using active interaction sources including Textmining, Experiments, Databases, and Co-expression. Next, the network, consisting of 61 nodes and 12 edges, was imported into Cytoscape software (v3.10.1), and three different algorithms of CytoHubba20, including Closeness, Clustering Coefficient, and Maximal Clique Centrality, were applied to screen out the hub genes [19, 20].

Validation of the hub genes

The identified hub genes were validated using the AAA datasets GSE57691 and GSE232911 and the RA datasets GSE1919 and GSE55457. A p-value of < 0.05 was defined as the threshold of significance. In addition, to evaluate the ability of these hub genes to predict disease accuracy, receiver operating characteristic curve (ROC) curves were plotted for the above four datasets by using the pROC package(v1.18.0) in R software (v4.2.2) [21].

Identification of key immune cells and correlation with genes

The immune cell composition involved in the co-pathogenesis of AAA and RA was determined using CIBERSORT (https://cibersort.stanford.edu/). In addition, we screened key immune infiltrating cells and evaluated their correlation with the hub genes. Visualization plots were generated using R software (v4.2.2), considering an adjusted p-value < 0.05 as the threshold of significance.

Identification of diseases, miRNAs, and TFs associated with the hub genes

The hub genes were imported into NetworkAnalyst (version 3.0, https://www.networkanalyst.ca/) and evaluated for their association with various diseases, miRNAs, and TFs. NetworkAnalyst is a comprehensive database for genetic analysis.

Identification of potential drugs

The hub genes were imported into the Enrichr database (https://maayanlab.cloud/Enrichr/), and the Drug Signatu re Database (DSigDB, http://tanlab.ucdenver.edu/DSigDB) was used to identify potential drugs and drug targets associated with the hub genes.

Validation of key immune cells

By collecting Immune cells in the blood from AAA patients, RA patients, and healthy individuals, the differences in immune cells in the blood of AAA patients and healthy individuals and RA patients and healthy individuals were analyzed, and the key immune cells were verified, with a p-value < 0.05 as the threshold of significance.

Statistical analysis

Continuous variables were first tested for normality using the Shapiro–Wilk test. Normally distributed data were expressed as mean ± standard deviation and compared using Student's t-test. Non-normally distributed data were expressed as median and compared using the Mann–Whitney U test. Categorical variables were compared using the chi-square (χ^2) test or Fisher's exact test, as appropriate. All statistical analyses were performed using SPSS (v27.0). A two-sided p-value < 0.05 was considered statistically significant.

Results

Identification of DEGs

The GSE47472 dataset for AAA contained data from 14 experimental group samples and 8 control group samples, comprising 351 upregulated and 577 downregulated DEGs. The RA dataset GSE97779 contained data from 9 experimental group samples and 5 control group samples and included 2175 upregulated and 2308 downregulated DEGs. After the data from the two datasets were combined, 61 common DEGs were identified, including 20 upregulated genes and 41 downregulated genes (Fig. 2). The distribution of logFC for common DEGs in the AAA and RA datasets is shown in Fig. S1.

Enrichment analysis of DEGs

The DEGs identified from the GSE47472 dataset and the GSE97779 dataset were subjected to separate GO and KEGG enrichment analyses. Subsequently, GO, KEGG, and DO enrichment analyses were conducted for the

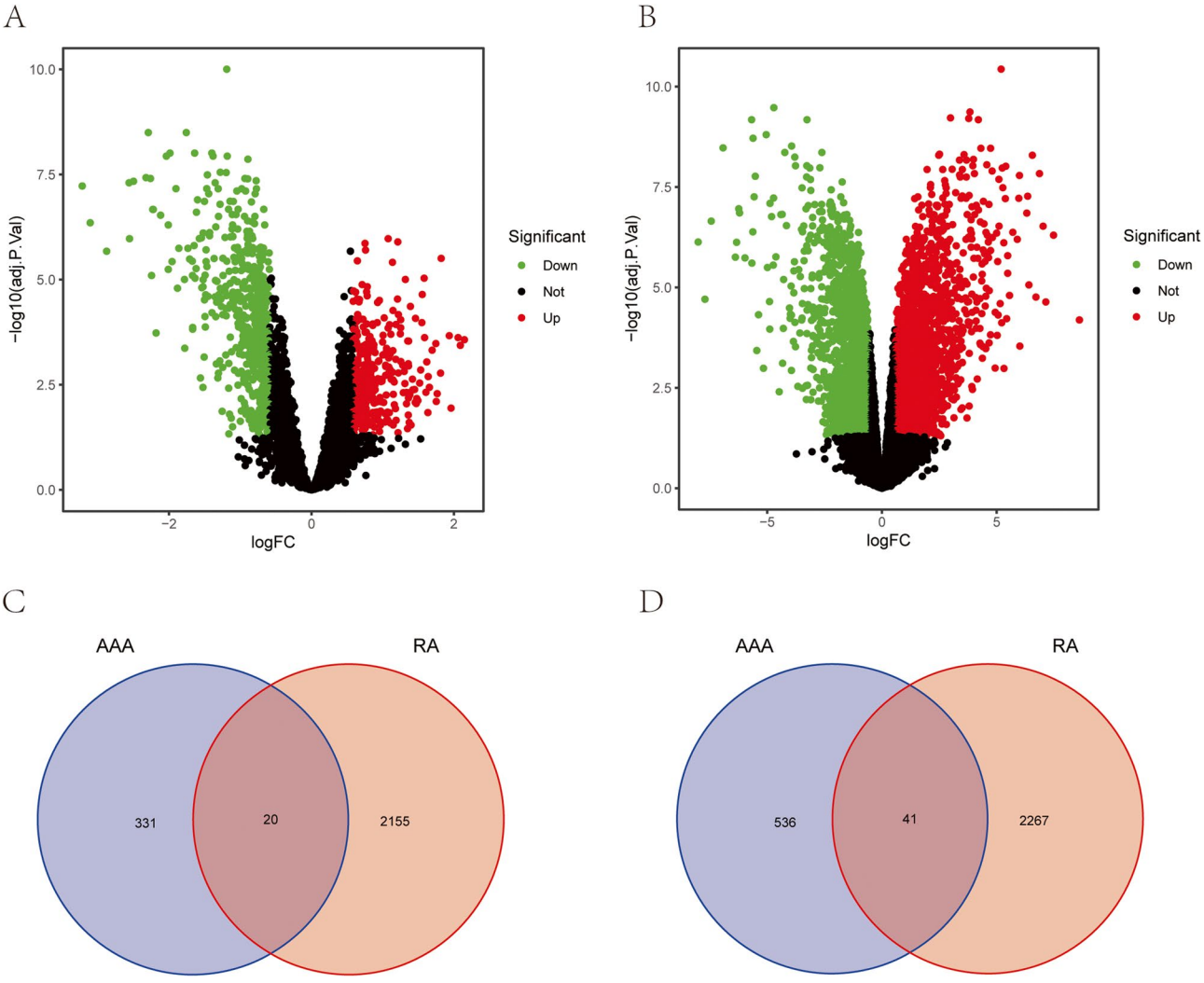


Fig. 2 Identification of DEGs. **A** 351 upregulated and 577 downregulated genes between AAA patients and healthy individuals. **B** 2175 upregulated and 2308 downregulated genes between RA patients and healthy individuals. **C** Twenty common upregulated DEGs between AAA and RA patients were identified by a Venn diagram. **D** Forty-one common downregulated DEGs between AAA and RA patients were identified by a Venn diagram

common DEGs identified between the two datasets. GO enrichment analysis of the AAA dataset revealed the following biological processes (BPs) in the top three ranks: metabolic processes involving the negative regulation of small molecules, retinal cone cell development, and retinal cone cell differentiation. In addition, the three highest ranked cellular components (CCs) were revealed and were as follows: acrosomal vesicle, U2-type precatalytic spliceosome, and precatalytic spliceosome. The three highest ranked molecular functions (MFs) were protein transporter activity, protein transmembrane transporter activity, and nonmembrane spanning protein tyrosine kinase activity. KEGG enrichment analysis of this dataset revealed the following as the top three pathways: cholesterol metabolism, cardiac muscle contraction, and steroid hormone biosynthesis (Fig. 3A, B). GO enrichment analysis of the RA dataset revealed the following as the top three BPs: leukocyte cell–cell adhesion, positive regulation of cytokine production, and myeloid leukocyte activation. In addition, the top three CCs were identified as follows: the cytoplasmic vesicle lumen, secretory granule lumen, and vesicle lumen. The top three MFs identified were immune receptor activity, cytokine receptor activity, and phosphatidylinositol 3-kinase regulator activity. KEGG enrichment analysis of this dataset revealed the following as the top three pathways: osteoclast differentiation, lysosome, and efferocytosis (Fig. 3C, D). GO enrichment analysis of the common DEGs revealed the following BPs as the top three terms: regulation of bone resorption, regulation of bone remodeling, and tissue homeostasis. In addition, the following were revealed as the top three CCs: the transcription elongation factor complex, histone deacetylase complex, and spindle microtubule. The three identified MFs were

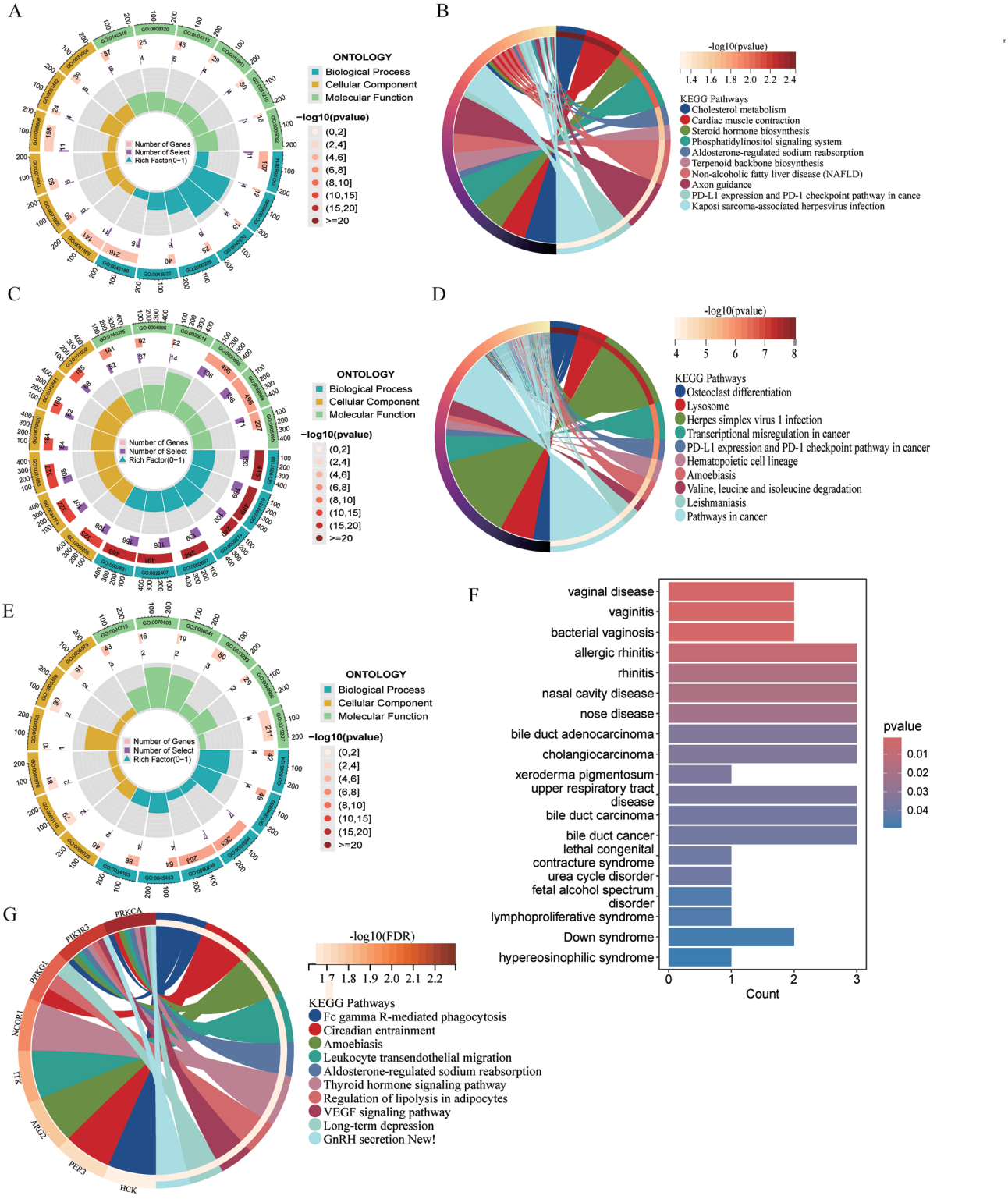


Fig. 3 Enrichment analysis (GO, KEGG, and DO) of the DEGs. **A**-**B** Enrichment analysis for DEGs from the AAA dataset. **C**-**D** Enrichment analysis for DEGs from the RA dataset. **E**-**G** Enrichment analysis of the common DEGs

nonmembrane spanning protein tyrosine kinase activity, NAD + binding, and long-chain fatty acid binding. KEGG enrichment analysis of the common DEGs revealed the following three pathways: Fc gamma R-mediated phagocytosis, circadian entrainment, and amoebiasis. DO enrichment analysis of the common DEGs revealed the following three diseases associated with these common DEGs: vaginal disease, vaginitis, and bacterial vaginosis (Fig. 3E, F, G).

Identification of candidate hub genes

A protein–protein interaction network of 61 common DEGs was constructed using the STRING database. Next, the CytoHubba algorithm was applied, and four genes were selected based on the results (Fig. 4A, B, C). By taking the intersection and constructing a Venn diagram, three candidate hub genes were identified, namely, ITK, CSK, and HCK (Fig. 4D). The expression of all three hub genes elevated in both the AAA and RA test cohorts.

Validation of the hub genes

The three candidate hub genes identified in the above steps were validated using the GSE57691 and GSE232911 datasets for AAA and the GSE1919 and GSE55457 datasets for RA. The results revealed that only ITK was consistently upregulated across all four datasets (Fig. 5). The ROC curves of the ITK showed that the AUC was > 0.7 in all four validation datasets, suggesting that the ITK can be considered a potential marker for predicting these two diseases (Fig. S2).

Identification of correlations between hub genes and immune-infiltrating cells

The CIBERSORT algorithm was applied to analyze the differences in the proportions of 22 immune cells between the AAA and RA cohorts, and the results were visualized using a bar graph (Fig. 6A, B). Violin plots were also generated for the results, and according to these plots, an increase in monocytes was indicated in both datasets, which suggested that monocytes were significantly correlated with both AAA and RA (Fig. 6C, D). Therefore, the correlation between ITK and monocytes

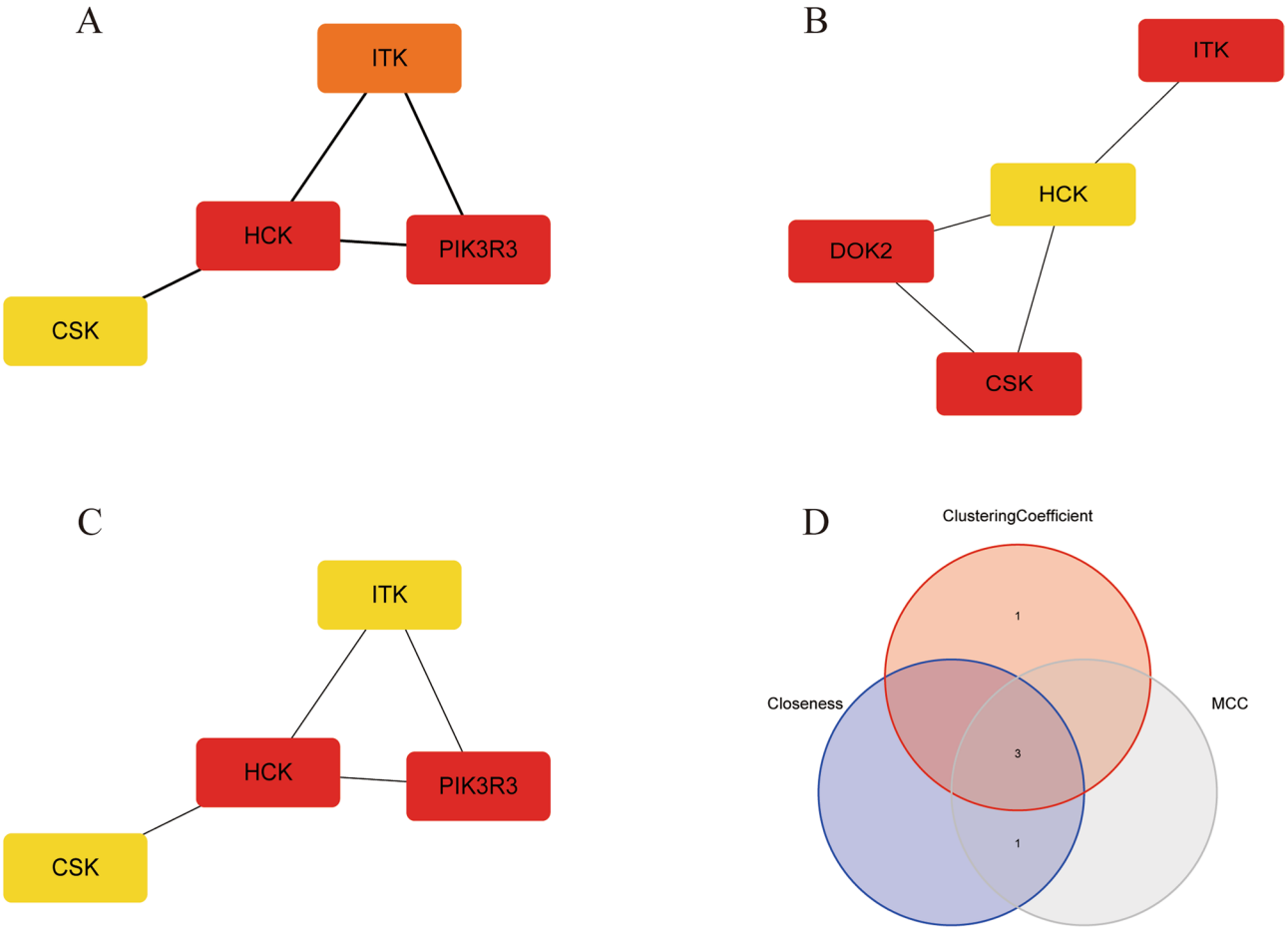


Fig. 4 Identification of candidate hub genes. **A** Closeness algorithm. **B** Clustering coefficient algorithm. **C** MCC algorithm. **D** The 3 common candidate hub genes screened out based on the Venn diagram

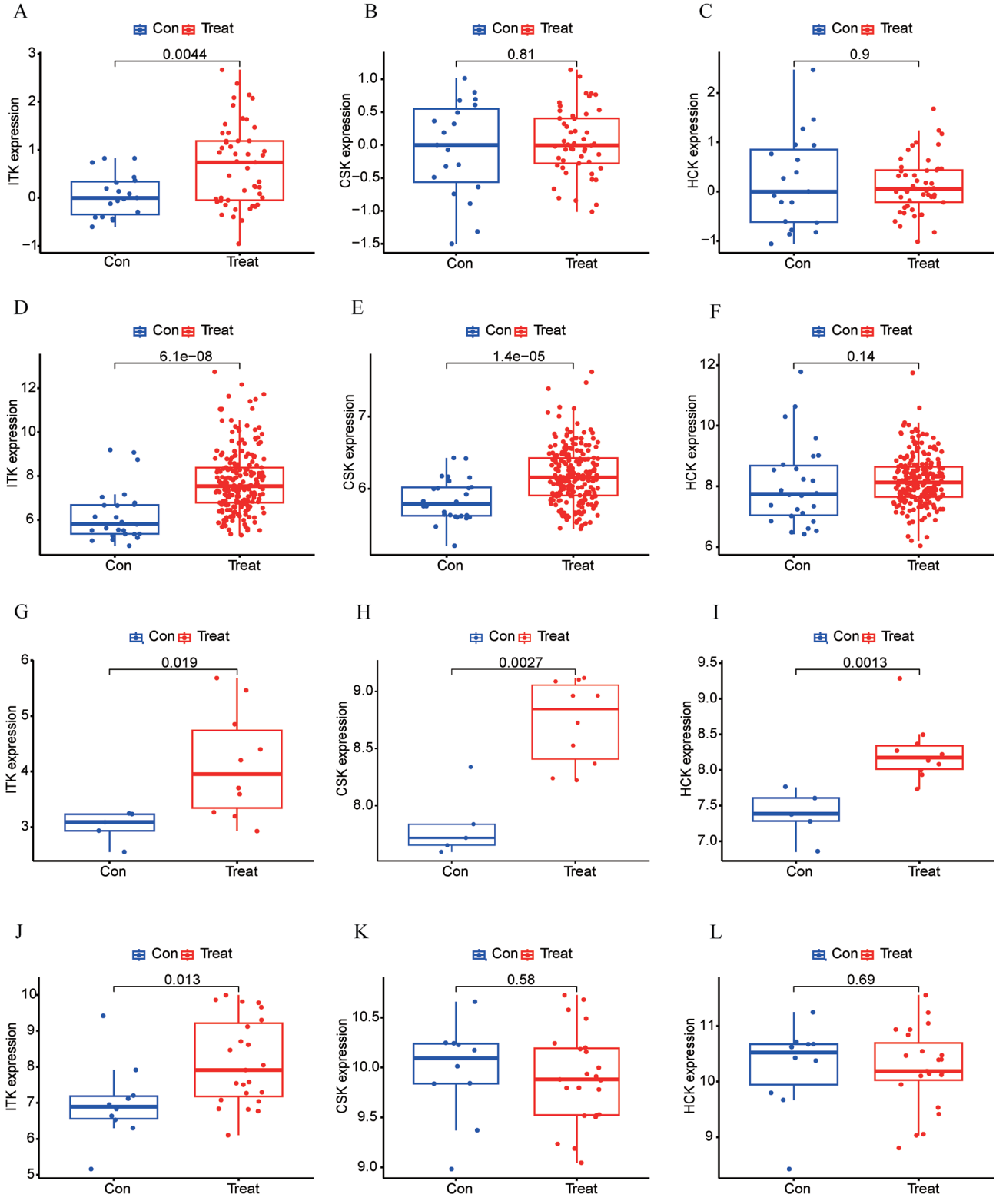


Fig. 5 Validation of the identified hub genes. **A**-**C** In AAA dataset GSE57691: ITK was significantly upregulated. **D**-**F** In AAA dataset GSE232911: ITK and CSK were upregulated. **G**-**I** In RA dataset GSE1919: ITK, CSK, and HCK were upregulated. **J**-**L** In RA dataset GSE55457: ITK was upregulated

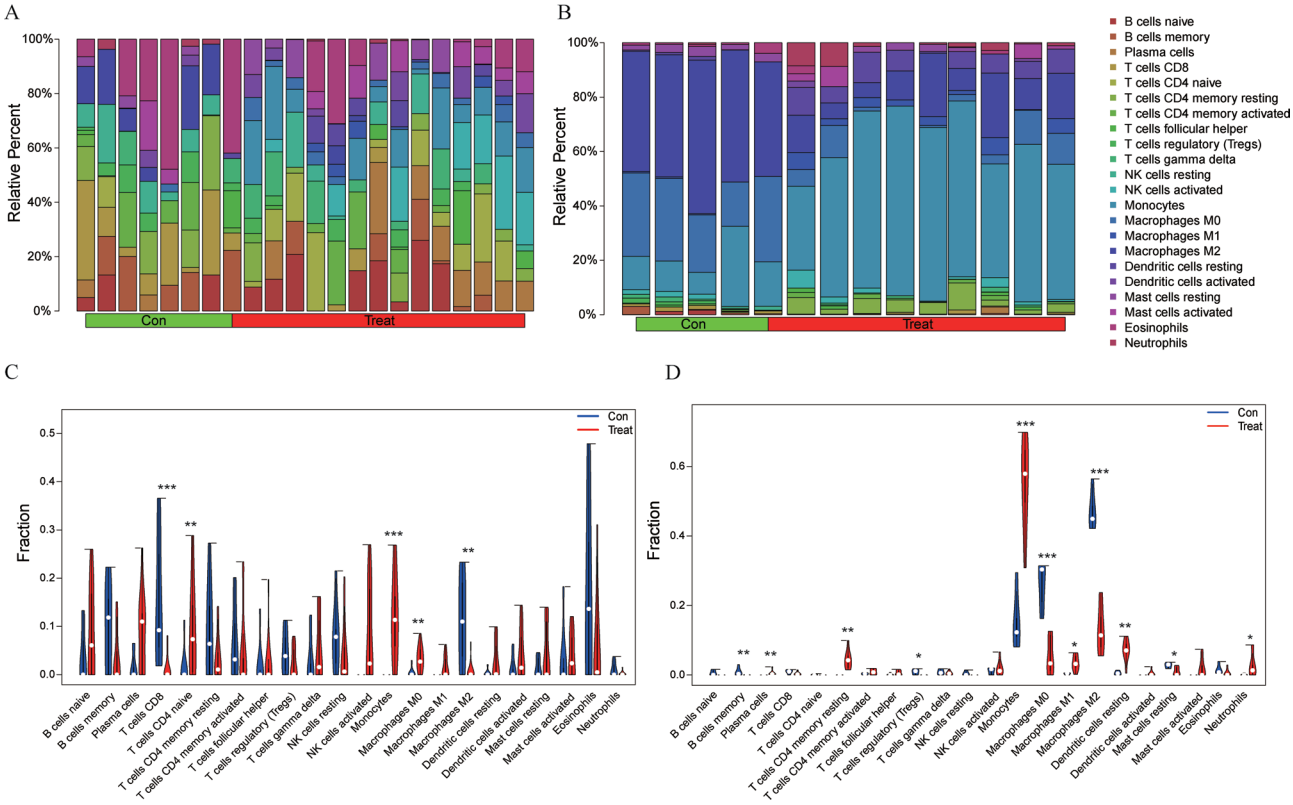


Fig. 6 Different immune cell types in the AAA and RA datasets. **A**-**B** Immune cell distribution visualized as a bar plot in AAA and RA datasets. **C**-**D**) Immune cell distribution visualized as a violin plot in AAA and RA datasets. * represents $P < 0.05$, ** represents $P < 0.01$, *** represents $P < 0.001$

was analyzed, and the results showed a significant positive correlation between ITK and monocytes, indicating that upregulation of ITK can cause increased immune infiltration of monocytes (Fig. 7A, B). A lollipop plot was subsequently generated, which further confirmed the correlation between ITK and monocytes (Fig. 7C, D).

Hub genes and immune cells identified by scRNA-seq

We performed scRNA-seq analyses on datasets from patients with AAA (4 samples and 2 controls) and RA (4 samples and 5 controls) using Seurat. Based on specific marker genes and uniform manifold approximation and projection (UMAP) dimensionality reduction, we successfully annotated a total of 11 major cell types, including monocytes (Fig. 8A, B). Subsequent analysis revealed that compared to controls, CD4 naïve T cell, monocyte, naïve B cells, and NK cell clusters were significantly expanded in the AAA group (Fig. 8C). In the RA samples, fibroblast, monocyte, and neutrophils clusters were all significantly expanded (Fig. 8D). Notably, monocyte cluster expansion was observed in both AAA and RA. We then assessed the expression patterns of three candidate hub genes (ITK, HCK, and CSK) across annotated cell clusters. The results showed that ITK was markedly upregulated in monocyte clusters of both AAA and RA samples compared with controls (Fig. 8E, F).

To further explore the functional features of ITK-high expressing cell populations, we performed GO and KEGG pathway enrichment analyses on their DEGs. GO enrichment in AAA revealed significant involvement in cytoplasmic translation, ribosome biogenesis, and protein–RNA complex assembly, as well as immune-related processes such as monocyte migration, chemotaxis, and regulation of inflammatory responses (Fig. S3A, B). In RA, differentially expressed genes were mainly enriched in biological processes related to post-transcriptional regulation, protein synthesis, and cell adhesion (Fig. S3C, D). KEGG pathway analysis showed that the top three significantly enriched pathways in AAA were T cell receptor signaling pathway, monocyte migration, and human T-cell leukemia virus 1 infection. In RA, the top enriched pathways were coronavirus disease-COVID-19, monocyte migration, and herpes simplex virus 1 infection. Importantly, "monocyte migration" was among the top pathways in both AAA and RA.

Identification of diseases, miRNAs, and TFs associated with the hub genes

The ITK gene was imported into NetworkAnalyst, and a network was constructed for the interactions of ITK with different miRNAs, TFs, and diseases. The analysis revealed eighteen diseases, ten miRNAs, and eight TFs

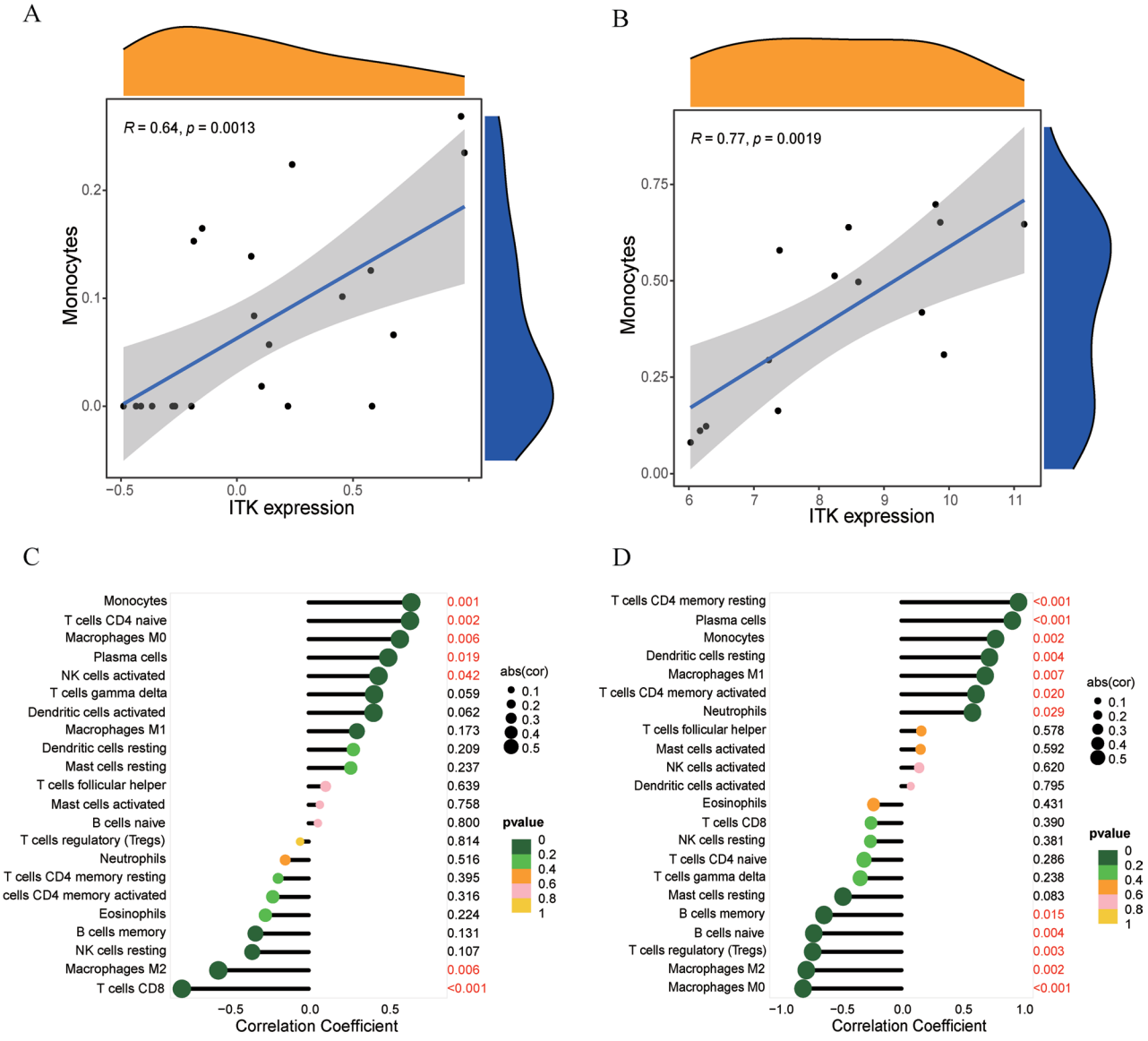


Fig. 7 Correlation between ITK and monocyte counts. **A**-**B** Correlation plot between ITK and monocyte counts in the AAA and RA datasets. **C**-**D** Lollipop plot between ITK and monocyte counts in the AAA and RA datasets

related to ITK. Notably, the eighteen diseases associated with ITK included autoimmune diseases (Fig. S4A).

Evaluation of potential drugs

The ITK gene was imported into the Enrichr database, and the drugs and drug targets associated with the hub genes were screened from the DSigDB. The top 10 drugs and targets related to the ITK were then selected according to the p-value ranking as potential drugs and targets suitable for use in treating ITK-related diseases (Fig. S4B).

Clinical data analysis

The clinical data of AAA patients, RA patients, and healthy individuals, including sex, age, platelet count, erythrocyte count, hemoglobin level, and immune cell counts, were collected. The results are listed in Tables S1 , S2 and S3. Sex, age, hemoglobin level, monocyte level, and lymphocyte level were significantly different between AAA patients and healthy individuals (Table S1). On the other hand, sex, platelet count, and the levels of basophils, eosinophils, monocytes, lymphocytes, neutrophils, and leukocytes differed significantly ($p < 0.05$) between RA patients and healthy individuals (Table S2). Subsequent univariate and multivariate binary logistic regression analyses of these significantly different immune cells revealed that monocyte counts were correlated with both AAA and RA (Table S3, S4).

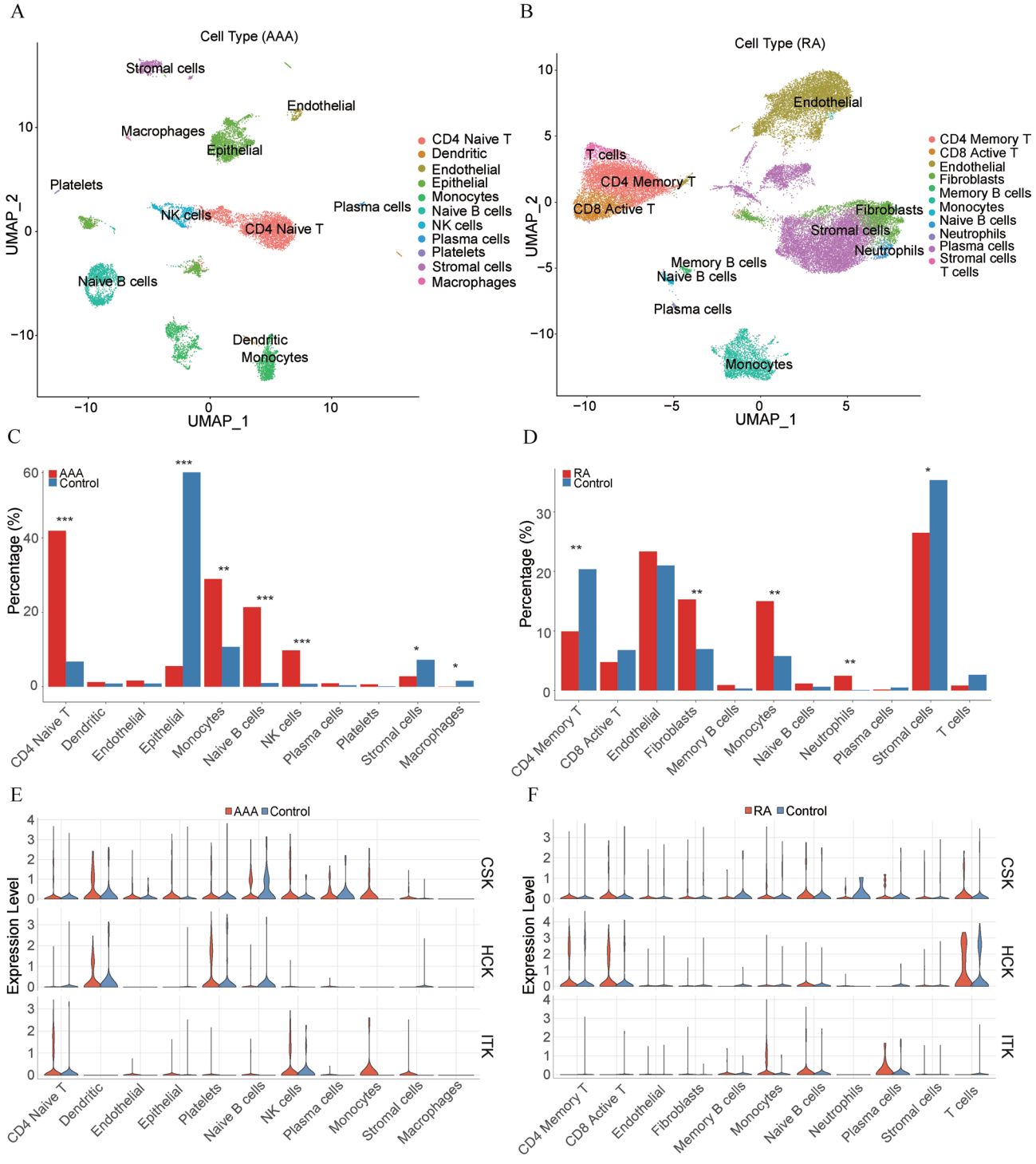


Fig. 8 **A**-**B** UMAP visualization of the AAA and RA scRNA-seq datasets. **C**-**D** Cellular composition in AAA, RA, and their respective control groups. **E**-**F** Expression of hub genes across different cell types in AAA and RA. * represents $P < 0.05$, ** represents $P < 0.01$, *** represents $P < 0.001$

Discussion

Previous studies have shown that RA might accelerate atherosclerosis, leading to arterial wall inflammation and an increased incidence of AAA [10, 22, 23]. However, the underlying mechanisms remain to be elucidated. In this study, we obtained transcriptomic data for both AAA and RA from the GEO database and performed integrated bioinformatics analyses to identify hub genes and patterns of immune cell infiltration. Our results suggest that both ITK and monocytes may play important roles in the

common pathogenic mechanisms underlying AAA and RA. Furthermore, we constructed a regulatory network for ITK, incorporating associated diseases, miRNAs, transcription factors, and potential drugs and drug targets, which may offer useful insights for future research.

ITK is a non-receptor tyrosine kinase predominantly expressed in T cells [24]. It has been reported to regulate the expression of pro-inflammatory cytokines by modulating the T-cell receptor, which plays a significant role in the inflammatory process [25, 26]. Moreover, studies have shown that ITK regulates the balance between pro-inflammatory T helper cells and anti-inflammatory regulatory T cells through Ca^{2+} signaling, thereby promoting the development of inflammation [27]. An increasing number of studies indicate that ITK signaling plays an important role in tumor development, autoimmune diseases, allergic diseases, and infectious diseases [28, 29]. In recent years, ITK inhibitors have been used for treating the above diseases, and promising outcomes have been achieved [25, 30]. Monocytes are well recognized to play key roles in various immune and inflammatory responses. However, research exploring the correlation between ITK and monocytes is currently limited. Notably, Sanjay Varikuti found that injection of ITK inhibitors in mice infected with leishmaniasis reduced monocyte infiltration in these mice, suggesting a potential correlation between ITK and monocytes during the inflammatory response [31].

It has been shown that the development of AAA is associated with autoimmunity and inflammation [32]. Although ITK has been demonstrated to contribute to autoimmune diseases through the regulation of signaling pathways within immune cells in various diseases, such as multiple sclerosis, inflammatory bowel disease, and systemic lupus erythematosus, its role in AAA remains poorly understood and has not been investigated [25, 33–35]. In recent years, research exploring the association between ITK and autoimmune diseases has progressed significantly, and the study of the association between ITK and the pathogenesis of AAA is expected to constitute a prospective direction for this field of research. Recently, a study on Kawasaki disease suggested that ITK may regulate the expression of $CD14^{+}$ monocytes, implicating a potential role in vascular inflammation [36]. Evidence suggests that monocytes are involved in the development of AAA and play an active role in vascular inflammation and vascular remodeling [37]. Our scRNA-seq analysis of AAA revealed that ITK-high expressing cell populations were significantly enriched in the T cell receptor signaling pathway and other inflammation-related pathways, suggesting that ITK-mediated inflammatory responses may play a contributory role in the pathogenesis of AAA. In separate murine studies, Marie Vandestienne and Safa Mellak observed that monocytes, under the influence of angiotensin II-mediated upregulation of CD62L and chemokines, infiltrate the mouse aortic wall, where these cells promote inflammatory responses, thereby contributing to the development and exacerbation of AAA in the mouse [38, 39]. Moreover, studies conducted with both AAA patients and healthy individuals revealed increased activation, endothelial adhesion, and migration of monocytes in AAA patients and a correlation between monocyte behavior and AAA diameter [40].

RA is the most common autoimmune disease [41]. ITK signaling is reported to negatively regulate Treg cells and positively regulate Th17 cells, resulting in an increase in pro-inflammatory Th17 cells and thereby contributing to the onset of RA [28, 42]. In this context, ITK has been shown to promote the generation of pro-inflammatory T helper cells and exacerbate inflammation in RA via the Akt-mTOR signaling pathway [43]. Ye et al. reported that inhibiting ITK could reduce the production of pathogenic Th17 cells while increasing the number of Treg cells, potentially ameliorating the symptoms of arthritis in patients [44]. Currently, various ITK inhibitors are used in the clinical treatment of AA patients, with promising results [25, 45]. The inflammatory factors involved in RA are produced mainly by monocytes. The inflammatory factors TNFα, IL-6, and IL-1 promote the polarization of Th17 cells via CD4 + T cells, leading to endothelial cell activation, an inflammatory response, and cartilage damage, which contribute to the development of RA [46–48]. In addition, circulating monocytes that transform into osteoclasts may directly cause bone destruction within the joint cavity [48]. Consistent with previous studies, our results suggest that ITK and monocytes are actively involved in the development of RA. Consistent with previous studies, our enrichment analysis also indicated that ITK may contribute to the development of RA by activating inflammation-related immune cell populations, including pathways such as T cell receptor signaling and monocyte migration.

We found that the miRNAs, diseases, and transcription factors associated with ITK are mostly related to inflammatory processes. For instance, miR-155-5p and miR-21-3p are well-known regulators of inflammatory responses [49, 50]. Diseases such as autoimmune disorders, aphthous stomatitis, and lymphoproliferative syndromes are also linked to chronic inflammation [51, 52]. In addition, TFs like STAT6, RUNX1, and FLI1 play critical roles in inflammatory signaling pathways [53, 54]. Although these findings provide valuable hypotheses for the regulatory mechanisms and potential therapeutic targets of ITK, it should be emphasized that these conclusions are based on correlation analysis and require further experimental validation, such as using CRISPR/Cas9-generated ITK-knockout cells to establish genetic

models, ITK 3'UTR luciferase assays for miRNA-ITK targeting validation, Co-immunoprecipitation to confirm ITK-transcription factor interactions, and disease-relevant immune phenotyping in T cell-specific ITK conditional knockout mice.

This study has several limitations. First, due to data limitations, the analysis was restricted to patients with either AAA or RA, without concurrent evaluation of data from patients diagnosed with both conditions. Second, the common DEGs selected in this study are based on consistent regulatory directions, which may overlook genes that exhibit opposite directions in the two diseases but still hold biological significance. Additionally, the validation step focused only on key immune cells associated with the diseases, while no experimental validation was performed for the identified hub genes. Future studies should conduct fundamental research to explore the relationship between ITK and both AAA and RA.

Conclusions

Our findings suggest that ITK may participate in the shared pathogenesis of AAA and RA, with monocytes contributing significantly to the inflammatory processes in both diseases. Accordingly, we constructed a preliminary regulatory network centered on ITK and identified related miRNAs, diseases, TFs, and potential drugs and drug targets, which may provide potential value for future research.

Abbreviations

AAA	Abdominal aortic aneurysm
RA	Rheumatoid arthritis
GEO	Gene Expression Omnibus
scRNA-seq	Single-cell RNA sequencing
DEGs	Differentially expressed genes
GO	Gene Ontology
KEGG	Kyoto Encyclopedia of Genes and Genomes
DO	Disease Ontology
UMAP	Uniform manifold approximation and projection
DSigDB	Drug Signature Database
TFs	Transcription factors
ROC	Receiver operating characteristic curve
BPs	Biological processes
CCs	Cellular components
MFs	Molecular functions

Supplementary Information

The online version contains supplementary material available at https://doi.org/10.1186/s12920-025-02236-y.

Supplementary Material 1.

Supplementary Material 2.

Supplementary Material 3.

Acknowledgements

We thank Dr. Xiao Qin, for his constant support and motivation.

Authors' contributions

YW and LZ designed the research, analyzed the data, wrote the paper, and revised the manuscript. QK and WJ analyzed the data. XQ revised the paper. All authors have given approval to the final version of the manuscript.

Funding

This work was supported by the National Natural Science Foundation of China: 81960091, and Prof. Xiao qin from the First Affiliated Hospital of Guangxi Medical University is the recipient.

Data availability

The datasets used or analyzed during the current study are available from GEO repository: [https://www.ncbi.nlm.nih.gov/geo/](https:/www.ncbi.nlm.nih.gov/geo). Other data generated or analyzed during this study are included in this published article.

Declarations

Ethics approval and consent to participate

This study was approved by the Ethics Committee of The First Affiliated Hospital of Guangxi Medical University (approval number: 2024-E007-01). Written informed consent was obtained from individual participants.

Consent for publication

Not applicable.

Competing interests

The authors declare no competing interests.

Author details

[1]Department of Vascular Surgery Ward, The First Affiliated Hospital of Guangxi Medical University, Nanning 530000, Guangxi, China
[2]Department of Vascular Surgery Ward, The Fourth Affiliated Hospital of Guangxi Medical University, Liuzhou 545000, Guangxi, China

Received: 20 June 2024 / Accepted: 12 September 2025
Published online: 09 October 2025

References

1. Baman JR, Eskandari MK. What is an abdominal aortic aneurysm? JAMA. 2022;328(22):2280. https://doi.org/10.1001/jama.2022.18638.
2. Sakalihasan N, Limet R, Defawe OD. Abdominal aortic aneurysm. Lancet. 2005;365(9470):1577–89. https://doi.org/10.1016/s0140-6736(05)66459-8.
3. Márquez-Sánchez AC, Koltsova EK. Immune and inflammatory mechanisms of abdominal aortic aneurysm. Front Immunol. 2022;13:989933. https://doi.org/10.3389/fimmu.2022.989933.
4. Hellenthal FA, Buurman WA, Wodzig WK, Schurink GW. Biomarkers of abdominal aortic aneurysm progression. Part 2: inflammation. Nat Rev Cardiol. 2009;6(8):543–52. https://doi.org/10.1038/nrcardio.2009.102.
5. Smolen JS, Aletaha D, McInnes IB. Rheumatoid arthritis. Lancet. 2016;388(10055):2023–38. https://doi.org/10.1016/s0140-6736(16)30173-8.
6. McInnes IB, Schett G. The pathogenesis of rheumatoid arthritis. N Engl J Med. 2011;365(23):2205–19. https://doi.org/10.1056/NEJMra1004965.
7. van Delft MAM, Huizinga TWJ. An overview of autoantibodies in rheumatoid arthritis. J Autoimmun. 2020;110:102392. https://doi.org/10.1016/j.jaut.2019.102392.
8. Derksen V, Huizinga TWJ, van der Woude D. The role of autoantibodies in the pathophysiology of rheumatoid arthritis. Semin Immunopathol. 2017;39(4):437–46. https://doi.org/10.1007/s00281-017-0627-z.
9. England BR, Thiele GM, Anderson DR, Mikuls TR. Increased cardiovascular risk in rheumatoid arthritis: mechanisms and implications. BMJ. 2018;361:k1036. https://doi.org/10.1136/bmj.k1036.
10. Shovman O, Tiosano S, Comaneshter D, Cohen AD, Amital H, Sherf M. Aortic aneurysm associated with rheumatoid arthritis: a population-based cross-sectional study. Clin Rheumatol. 2016;35(11):2657–61. https://doi.org/10.1007/s10067-016-3372-0.
11. Figus FA, Piga M, Azzolin I, McConnell R, Iagnocco A. Rheumatoid arthritis: Extra-articular manifestations and comorbidities. Autoimmun Rev. 2021;20(4):102776. https://doi.org/10.1016/j.autrev.2021.102776.

12. Shen Y, Gao Y, Shi J, Huang Z, Dai R, Fu Y, et al. MicroRNA-disease network analysis repurposes methotrexate for the treatment of abdominal aortic aneurysm in mice. Genomics Proteom Bioinf. 2023;21(5):1030–42. https://doi.org/10.1016/j.gpb.2022.08.002.
13. Ritchie ME, Phipson B, Wu D, Hu Y, Law CW, Shi W, et al. Limma powers differential expression analyses for RNA-sequencing and microarray studies. Nucleic Acids Res. 2015;43(7):e47. https://doi.org/10.1093/nar/gkv007.
14. Jia A, Xu L, Wang Y. Venn diagrams in bioinformatics. Brief Bioinform. 2021;22(5). https://doi.org/10.1093/bib/bbab108.
15. Cui CY, Liu X, Peng MH, Liu Q, Zhang Y. Identification of key candidate genes and biological pathways in neuropathic pain. Comput Biol Med. 2022;150:106135. https://doi.org/10.1016/j.compbiomed.2022.106135.
16. Gene Ontology Consortium. Gene ontology consortium: going forward. Nucleic Acids Res. 2015;43(Database issue):D1049–56. https://doi.org/10.1093/nar/gku1179.
17. Kanehisa M, Furumichi M, Sato Y, Kawashima M, Ishiguro-Watanabe M. KEGG for taxonomy-based analysis of pathways and genomes. Nucleic Acids Res. 2023;51(D1):D587–92. https://doi.org/10.1093/nar/gkac963.
18. Schriml LM, Munro JB, Schor M, Olley D, McCracken C, Felix V, et al. The human disease ontology 2022 update. Nucleic Acids Res. 2022;50(D1):D1255–61. https://doi.org/10.1093/nar/gkab1063.
19. Chin CH, Chen SH, Wu HH, Ho CW, Ko MT, Lin CY. CytoHubba: identifying hub objects and sub-networks from complex interactome. BMC Syst Biol. 2014;8(Suppl 4):S11. https://doi.org/10.1186/1752-0509-8-s4-s11.
20. Shannon P, Markiel A, Ozier O, Baliga NS, Wang JT, Ramage D, et al. Cytoscape: a software environment for integrated models of biomolecular interaction networks. Genome Res. 2003;13(11):2498–504. https://doi.org/10.1101/gr.1239303.
21. Robin X, Turck N, Hainard A, Tiberti N, Lisacek F, Sanchez JC, et al. pROC: an open-source package for R and S+to analyze and compare ROC curves. BMC Bioinformatics. 2011;12:77. https://doi.org/10.1186/1471-2105-12-77.
22. Carbone F, Bonaventura A, Liberale L, Paolino S, Torre F, Dallegri F, et al. Atherosclerosis in rheumatoid arthritis: promoters and opponents. Clin Rev Allergy Immunol. 2020;58(1):1–14. https://doi.org/10.1007/s12016-018-8714-z.
23. Agca R, Blanken AB, van Sijl AM, Smulders YM, Voskuyl AE, van der Laken C, et al. Arterial wall inflammation is increased in rheumatoid arthritis compared with osteoarthritis, as a marker of early atherosclerosis. Rheumatology (Oxford). 2021;60(7):3360–8. https://doi.org/10.1093/rheumatology/keaa789.
24. Fu Z, Huang Z, Xu H, Liu Q, Li J, Song K, et al. IL-2-inducible T cell kinase deficiency sustains chimeric antigen receptor T cell therapy against tumor cells. J Clin Invest. 2024;135(4). https://doi.org/10.1172/jci178558.
25. Lechner KS, Neurath MF, Weigmann B. Role of the IL-2 inducible tyrosine kinase ITK and its inhibitors in disease pathogenesis. J Mol Med (Berl). 2020;98(10):1385–95. https://doi.org/10.1007/s00109-020-01958-z.
26. Andreotti AH, Schwartzberg PL, Joseph RE, Berg LJ. T-cell signaling regulated by the tec family kinase, Itk. Cold Spring Harb Perspect Biol. 2010;2(7):a002287. https://doi.org/10.1101/cshperspect.a002287.
27. Anannya O, Huang W, August A. The kinase ITK controls a Ca(2+)-mediated switch that balances T(H)17 and T(reg) cell differentiation. Sci Signal. 2024;17(846):eadh2381. https://doi.org/10.1126/scisignal.adh2381.
28. Weeks S, Harris R, Karimi M. Targeting ITK signaling for T cell-mediated diseases. iScience. 2021;24(8):102842. https://doi.org/10.1016/j.isci.2021.102842.
29. Youssefian L, Vahidnezhad H, Yousefi M, Saeidian AH, Azizpour A, Touati A, et al. Inherited Interleukin 2-Inducible T-Cell (ITK) kinase deficiency in siblings with epidermodysplasia verruciformis and hodgkin lymphoma. Clin Infect Dis. 2019;68(11):1938–41. https://doi.org/10.1093/cid/ciy942.
30. Norman P. Inducible tyrosine kinase inhibitors: a review of the patent literature (2010–2013). Expert Opin Ther Pat. 2014;24(9):979–91. https://doi.org/10.1517/13543776.2014.936381.
31. Varikuti S, Volpedo G, Saljoughian N, Hamza OM, Halsey G, Ryan NM, et al. The potent ITK/BTK inhibitor ibrutinib is effective for the treatment of experimental visceral leishmaniasis caused by leishmania donovani. J Infect Dis. 2019;219(4):599–608. https://doi.org/10.1093/infdis/jiy552.
32. Huanggu H, Yang D, Zheng Y. Blood immunological profile of abdominal aortic aneurysm based on autoimmune injury. Autoimmun Rev. 2023;22(3):103258. https://doi.org/10.1016/j.autrev.2022.103258.
33. Xu WD, Su LC, Xie QB, Zhao Y, Liu Y. Interleukin-2-inducible T-cell kinase expression and relation to disease severity in systemic lupus erythematosus. Clin Chim Acta. 2016;463:11–7. https://doi.org/10.1016/j.cca.2016.10.010.
34. Lechner K, Mott S, Al-Saifi R, Knipfer L, Wirtz S, Atreya R, et al. Targeting of the tec kinase ITK drives resolution of T Cell-Mediated colitis and emerges as potential therapeutic option in ulcerative colitis. Gastroenterology. 2021;161(4):1270–e8719. https://doi.org/10.1053/j.gastro.2021.06.072.
35. Yin Z, Zou Y, Wang D, Huang X, Xiong S, Cao L, et al. Regulation of the tec family of non-receptor tyrosine kinases in cardiovascular disease. Cell Death Discov. 2022;8(1):119. https://doi.org/10.1038/s41420-022-00927-4.
36. Song S, Chen L, Zhou Y, Xu Y, Li G, Shen L, et al. CD14(+) monocytes: the immune communication hub in early vasculitis symptoms of Kawasaki disease. Front Immunol. 2025;16:1557231. https://doi.org/10.3389/fimmu.2025.1557231.
37. Raffort J, Lareyre F, Clément M, Hassen-Khodja R, Chinetti G, Mallat Z. Monocytes and macrophages in abdominal aortic aneurysm. Nat Rev Cardiol. 2017;14(8):457–71. https://doi.org/10.1038/nrcardio.2017.52.
38. Vandestienne M, Zhang Y, Santos-Zas I, Al-Rifai R, Joffre J, Giraud A, et al. TREM-1 orchestrates angiotensin II-induced monocyte trafficking and promotes experimental abdominal aortic aneurysm. J Clin Invest. 2021;131(2). https://doi.org/10.1172/jci142468.
39. Mellak S, Ait-Oufella H, Esposito B, Loyer X, Poirier M, Tedder TF, et al. Angiotensin II mobilizes spleen monocytes to promote the development of abdominal aortic aneurysm in Apoe-/- mice. Arterioscler Thromb Vasc Biol. 2015;35(2):378–88. https://doi.org/10.1161/atvbaha.114.304389.
40. Samadzadeh KM, Chun KC, Nguyen AT, Baker PM, Bains S, Lee ES. Monocyte activity is linked with abdominal aortic aneurysm diameter. J Surg Res. 2014;190(1):328–34. https://doi.org/10.1016/j.jss.2014.03.019.
41. Smith MH, Berman JR, What. Is Rheumatoid Arthritis? Jama. 2022;327(12):1194. https://doi.org/10.1001/jama.2022.0786.
42. Mamontov P, Eberwine RA, Perrigoue J, Das A, Friedman JR, Mora JR. A negative role for the interleukin-2-inducible T-cell kinase (ITK) in human Foxp3+TREG differentiation. PLoS ONE. 2019;14(4):e0215963. https://doi.org/10.1371/journal.pone.0215963.
43. Bishop EL, Gudgeon N, Fulton-Ward T, Stavrou V, Roberts J, Boufersaoui A, et al. TNF-α signals through ITK-Akt-mTOR to drive CD4(+) T cell metabolic reprogramming, which is dysregulated in rheumatoid arthritis. Sci Signal. 2024;17(833):eadg5678. https://doi.org/10.1126/scisignal.adg5678.
44. Chen Y, Liang R, Shi X, Shen R, Liu L, Liu Y, et al. Targeting kinase ITK treats autoimmune arthritis via orchestrating T cell differentiation and function. Biomed Pharmacother. 2023;169:115886. https://doi.org/10.1016/j.biopha.2023.115886.
45. Sahu N, August A. ITK inhibitors in inflammation and immune-mediated disorders. Curr Top Med Chem. 2009;9(8):690–703. https://doi.org/10.2174/156802609789044443.
46. Roberts CA, Dickinson AK, Taams LS. The interplay between Monocytes/Macrophages and CD4(+) T cell subsets in rheumatoid arthritis. Front Immunol. 2015;6:571. https://doi.org/10.3389/fimmu.2015.00571.
47. Hirose S, Lin Q, Ohtsuji M, Nishimura H, Verbeek JS. Monocyte subsets involved in the development of systemic lupus erythematosus and rheumatoid arthritis. Int Immunol. 2019;31(11):687–96. https://doi.org/10.1093/intimm/dxz036.
48. Iwamoto N, Kawakami A. The monocyte-to-osteoclast transition in rheumatoid arthritis: recent findings. Front Immunol. 2022;13:998554. https://doi.org/10.3389/fimmu.2022.998554.
49. Xu Y, Zhang C, Cai D, Zhu R, Cao Y. Exosomal miR-155-5p drives widespread macrophage M1 polarization in hypervirulent Klebsiella pneumoniae-induced acute lung injury via the MSK1/p38-MAPK axis. Cell Mol Biol Lett. 2023;28(1):92. https://doi.org/10.1186/s11658-023-00505-1.
50. Guzeldemir-Akcakanat E, Sunnetci-Akkoyunlu D, Balta-Uysal VM, Özer T, Işik EB, Cine N. Differentially expressed MiRNAs associated with generalized aggressive periodontitis. Clin Oral Investig. 2023;28(1):7. https://doi.org/10.1007/s00784-023-05404-5.
51. Song Y, Li J, Wu Y. Evolving Understanding of autoimmune mechanisms and new therapeutic strategies of autoimmune disorders. Signal Transduct Target Ther. 2024;9(1):263. https://doi.org/10.1038/s41392-024-01952-8.
52. Paskiewicz A, Niu J, Chang C. Autoimmune lymphoproliferative syndrome: A disorder of immune dysregulation. Autoimmun Rev. 2023;22(11):103442. https://doi.org/10.1016/j.autrev.2023.103442.
53. Zhou S, Zhao T, Chen X, Zhang W, Zou X, Yang Y, et al. Runx1 deficiency promotes M2 macrophage polarization through enhancing STAT6 phosphorylation. Inflammation. 2023;46(6):2241–53. https://doi.org/10.1007/s10753-023-01874-7.

54. Chen E, Wu J, Huang J, Zhu W, Sun H, Wang X, et al. FLI1 promotes IFN-γ-induced kynurenine production to impair anti-tumor immunity. Nat Commun. 2024;15(1):4590. https://doi.org/10.1038/s41467-024-48397-9.

Publisher's Note

Springer Nature remains neutral with regard to jurisdictional claims in published maps and institutional affiliations.